Author/s:
Lee, HY;Nelson, D;Yan, W;Crozier, KB;Bullock, J;Kim, S

Title:
Gap-Surface Plasmon-Enhanced Photoluminescence of InSe

Date:
2023-05

Citation:
Lee, H. Y., Nelson, D., Yan, W., Crozier, K. B., Bullock, J. & Kim, S. (2023). Gap-Surface Plasmon-Enhanced Photoluminescence of InSe. Physica Status Solidi (B): Basic Research, 260 (5), https://doi.org/10.1002/pssb.202200436.

Gap Surface Plasmon Enhanced Photoluminescence of InSe

Ha Young Lee[1], Damian Nelson[2], Wei Yan[1], Kenneth B. Crozier[1,2,3], James Bullock[1], Sejeong Kim[1,*]

[1]Department of Electrical and Electronic Engineering, University of Melbourne, Victoria 3010, Australia
[2]School of Physics, University of Melbourne, Victoria 3010, Australia
[3]Australian Research Council (ARC) Centre of Excellence for Transformative Meta-Optical Systems (TMOS), University of Melbourne, Victoria 3010, Australia

*sejeong.kim@unimelb.edu.au

Keywords: Gap surface plasmon, InSe, 2D materials, photoluminescence

Abstract

Two dimensional (2D) materials, with distinct characteristics compared to their conventional bulk counterparts, have been a popular topic in various optoelectronic research fields. In this report, we explore indium selenide (InSe), a monochalcogenide van der Waals layered semiconductor, which has been studied due to its thickness dependent optical characteristics. For InSe to be used as a versatile light source, enhancing the emission of InSe is required. Here, we demonstrate enhanced photoluminescence (PL) from multi-layer InSe using a gap plasmon induced between Ag nanocube dimer and an Au substrate. Such plasmonic structures support multiple resonances, one of those overlapping with InSe's band edge PL emission. The calculated Purcell factor shows a 200-fold increase on the short edge of nanocube dimers. Experimentally, PL enhancement of 6-fold is demonstrated at room temperature. In addition, we show a method of determining the thickness of 2D materials via dark-field spectroscopy using white light illumination. This study paves the way for the incorporation of 2D InSe into nanophotonic structures.

1. Introduction

Two dimensional (2D) materials have been widely studied in the last two decades for their unique properties compared to bulk materials.[1-4] For example, their layered nature allows easy integration with other optical components such as waveguides and cavities regardless of lattice matching.[2,5] Also, a growing library of 2D materials has been grown by processes such as chemical vapor deposition (CVD) [6,7] and atomic layer deposition (ALD)[8,9], allowing large area deposition and integration with existing CMOS processes.[10,11] Indium selenide (InSe) is a monochalcogenide semiconductor with a layered structure which is receiving significant research attention due to its favorable optical and electrical properties such as its nonlinear absorption properties in the mid-infrared region[12] and high carrier mobility at room temperature.[13-15] Like many other 2D materials, InSe also has bandgap tunability with respect to layer thickness.[16,17] InSe has a direct bandgap of 1.26 eV in its bulk form, which increases to 2.11 eV for monolayers owing to quantum confinement.[14,18,19] This presents an interesting research avenue, as it may have broadband PL emission tunability from the visible-to-near infrared (NIR) range (580-980 nm), opening up opportunities to control optical properties of 2D materials and their heterostructures in a wide range of PL spectrum.

However, despite these merits, there are some obstacles that need to be overcome to utilize InSe. Typical InSe has a relatively long radiative decay time (23.8 ns[20]), compared to other 2D materials such as transition metal dichalcogenides (TMDs), which have emission decay times of ~3-5 ps.[21,22] This relatively slow spontaneous emission rate needs to be overcome for InSe to be utilized in brighter PL and high frequency photonic and optoelectronic devices. Therefore, it is critical to shorten the lifetime of InSe for it to be used as an efficient on-chip light source. To control this emission property, this paper uses the gap surface plasmon enhanced cavity effect.[23,24] This utilizes a broad linewidth plasmonic resonator, having spectral overlap with the emitters, increasing the local density of states (LDOS)[25-27], which enhances the photoluminescence emission at InSe's band edge.

For InSe to have maximum emission enhancement from the cavity structure, polarization matching between the intrinsic luminescent exciton of InSe and the plasmon polarization of the cavity structure is needed. The intrinsic out-of-plane orientation of the InSe luminescent exciton[28] aligns well with metallic film-coupled metal nanocubes with a cavity in the middle, as the dominant plasmon polarization in this structure is also oriented perpendicular to the cavity layer[24]. Moreover, with the help of the layer stacking method, precise control of the gap thickness is possible in this structure. This comes to be an important factor, since the field enhancement occurs in the gap between two metals, the precise fabrication of the structure with two resonating metallic nanoparticles and nanoscale gap in the middle is critical.[23,29]

In this work, we focus on the gap mode-induced PL enhancement of InSe flakes. The structure consists of a mechanically exfoliated InSe flake (20-70 nm) sandwiched between a gold substrate and a silver nanocube dimer. Here we performed simulation and experimental analysis of an Au-InSe-Ag nanocube dimer (AIAN) structure to study the PL enhancement and the characteristics of the plasmonic modes. The AIAN structure is shown to have a 6-fold photoluminescence improvement compared to pristine InSe flake on the gold substrate. The structure studied in this paper expands the field of plasmon hybridized 2D materials in the visible-to-near-infrared region for optoelectronic and photonic applications.

2. Experimental Design

2.1. Simulation setup

The finite-difference time-domain (FDTD) method in the commercial software package from Lumerical (Lumerical Inc.) is used to simulate the electric field intensity distributions and spectra of gap plasmon mode. The simulations include a 100 nm thick Au substrate, a 25 nm thick InSe flake (n = 2.45[30]), and two Ag nanocubes. Each Ag nanocube has a length of 70 nm and is coated with a 2.5 nm[23] PVP layer (n = 1.4[24]). The edges of the nanocubes are rounded with a radius of 5 nm. The broadband plane wave light source is incident on top of the whole structure, normal to the surface of the substrate. The calculation was conducted at the spectral window at InSe's band edge PL (980 nm). For the far-field radiation pattern calculation, the monitor is located 90 nm above the structure, parallel to the Au substrate.

The commercial finite element method (FEM) solver, COMSOL Multiphysics (COMSOL Multiphysics 5.4) is used to calculate the Purcell factor. A spherical domain is created around an isolated nanocube dimer with second order scattering boundary conditions used to approximate an infinite domain. The nanocubes are modeled with a side length of 60 nm with a 1 nm PVP layer. The nanocubes are separated by a 0.6 nm air gap. An InSe layer of 23 nm is sitting on top of a 100 nm Au substrate. A monochromatic, vertically oriented electric dipole (980 nm) is positioned underneath the dimer inside the InSe layer, and its position is incrementally varied over a 15 x 30 grid. The Green's function of the system is calculated at each position underneath the dimer by evaluating the electric field due to the electric dipole at its current location. From this, the system's spontaneous emission rate is calculated and compared to that of an electric dipole radiating in free space.[31] The resulting heat map shows that the Purcell factor is highest in regions along the short edge of the dimer system, with maximum values of around 200.

2.2. Sample preparation

Sequential layers of 10 nm chromium and 100 nm gold are deposited onto SiO_2 (285 nm)/Si wafers using an electron beam evaporator (Thermionics VE180) with a deposition rate of 6 nm/min at 4 x 10^{-7} mbar. InSe flakes are mechanically exfoliated onto the gold surface at 60°C. A solution containing silver nanocubes (1 mg/mL in ethanol, PVP stabilized, nanoComposix) is diluted by a volume ratio of 1:50 with deionized water. This solution is then drop casted (5 µL) on the Au/InSe surface using a micropipette.

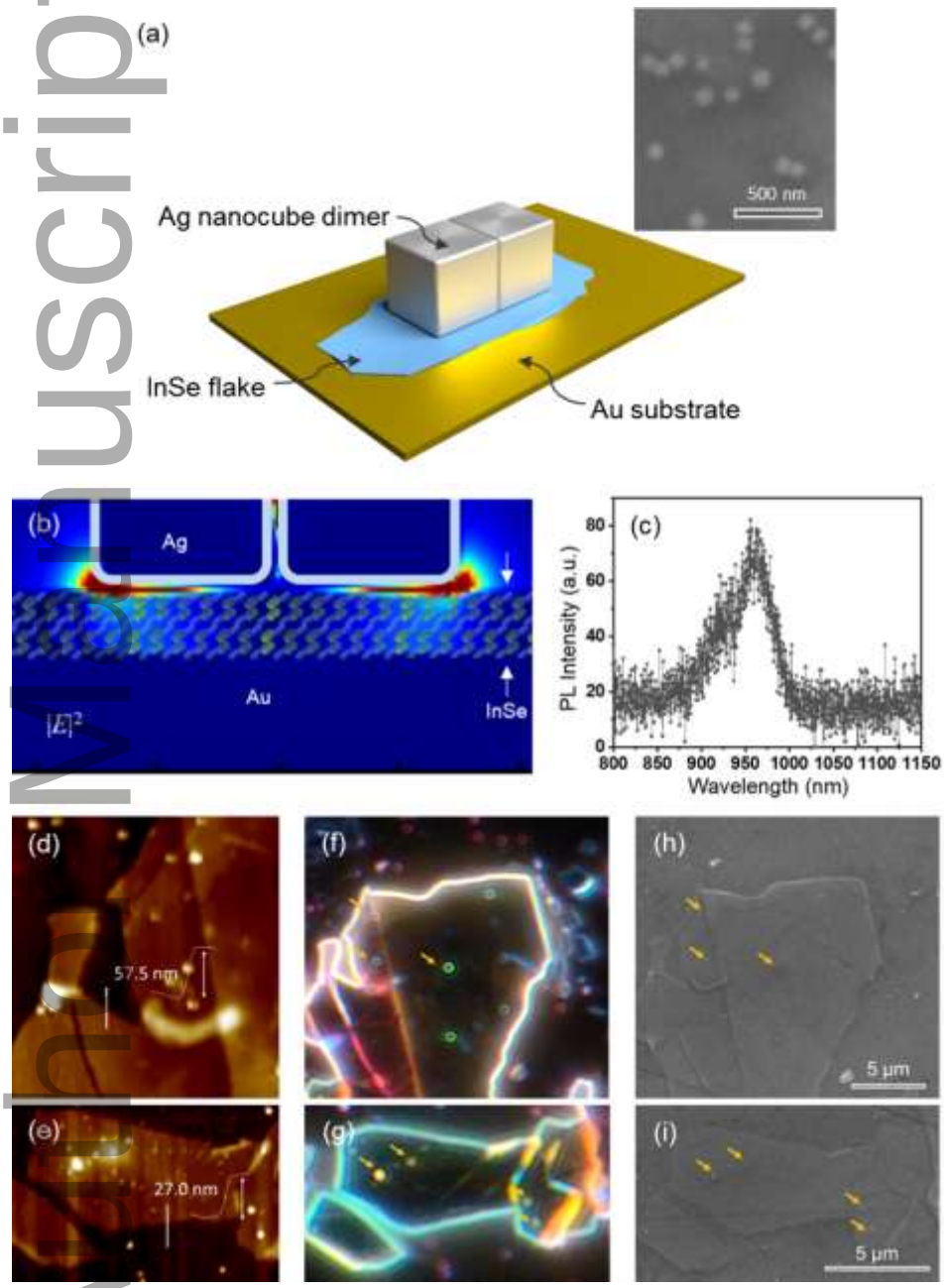

Figure 1. a) 3D schematic of Au substrate-InSe flake-Ag nanocube (AIAN). The inset shows a scanning electron microscope (SEM) image of Ag nanocubes on a InSe flake. b) A FDTD simulation result showing electric field intensity distribution at the gap. c) Photoluminescence spectrum of InSe on gold substrate. d, e) AFM images of InSe flakes with silver nanocubes on top, line scans of height steps are inset showing the thickness of flakes. f-i) Dark-field optical microscope images (f, g) and corresponding SEM images (h, i) of the sample in (d, e) respectively. Locations of some nanocubes are indicated with yellow arrows as guide points to show one-to-one matching between the dark field image and the SEM image.

3. Results and discussion

Figure 1a shows the AIAN structure consisting of an Au substrate, an InSe flake, and an Ag nanocube dimer. The inset shows the Ag nanocubes on the InSe flake, identified by scanning electron microscopy (SEM, Hitachi FlexSEM 1000). Single nanocubes, dimers and trimers can be found in the same InSe flake (Raman spectroscopy analysis of the InSe flake can be found in Fig. s1 of the supporting information[32,33]). **Figure 1b** shows the electric field intensity distribution of the gap mode induced by the AIAN structure. The structure consists of, from top to bottom, a silver nanocube dimer coated with PVP, 2D InSe with a thickness of 25 nm, and 100 nm gold substrate. The crystal structure of InSe[13,19] is overlapped in the gap area. The simulated plasmonic gap mode shows that the mode is localized in the gap region. Silver nanocube dimer structures with plasmonic resonance around 980 nm are used to have spectral overlap with the band edge PL of InSe. **Figure 1c** shows a PL spectrum from InSe without silver cubes.

The effect of InSe thickness is explored by surveying flakes of multiple thicknesses with appropriate Ag nanocubes. **Figure 1d&e** show atomic force microscopy (AFM, Asylum Research Cypher) images of the AIAN sample with different InSe thickness. The step profile line scan of each layer is indicated next to each white line. To avoid surface damage to the InSe flake, which may alter the luminescence properties, we first correlate features observed under dark-field OM with nanocube locations confirmed via SEM on test samples. **Figure 1f&i** show the comparison between the dark-field OM image and SEM image of the AIAN structure. The individual nanocubes are indicated with yellow arrows. These patterns are used to identify nanocube locations on subsequent samples. This one-to-one matching from dark-field image and SEM images navigates the facile and non-destructive method of distinguishing nanoparticles on thin films. **Figure 1f&g** shows the dark-field OM image of Ag nanocube on 40-70 nm, and ~20 nm thick (supporting information Fig. s2) InSe flakes, respectively. **Figure 1h&i** shows SEM images of the same flakes in **Figure 1d&e**, respectively. In dark-field optical microscopy, we observe donut-like shapes from metal particles on thicker films (40-70 nm) while appearing as Airy disk shapes from thinner films (~20 nm). Therefore, dark-field microscopy allows us a rapid estimation of InSe thickness roughly as well as the location of the metal nanocubes.

The samples are measured using a custom built confocal micro-PL setup at room temperature. A pulsed laser with a wavelength of 520 nm (3.89 MHz, 15 μW) is used in this experiment. An objective lens (100×, NA = 0.9) is used to focus the excitation laser and to collect the PL from the sample. The PL is passed through a 593 nm long-pass filter to remove the excitation laser beam. The PL beam is then coupled into single-mode optical fiber and is collected into the avalanche photodiode (APD, Excelitas Technologies). The filtered beam is also routed to a spectrometer (SpectraPro HRS-500, 150 g/mm) for spectral analysis. All samples are measured within one day of fabrication to minimize any oxidation of the InSe flake and silver nanocube.

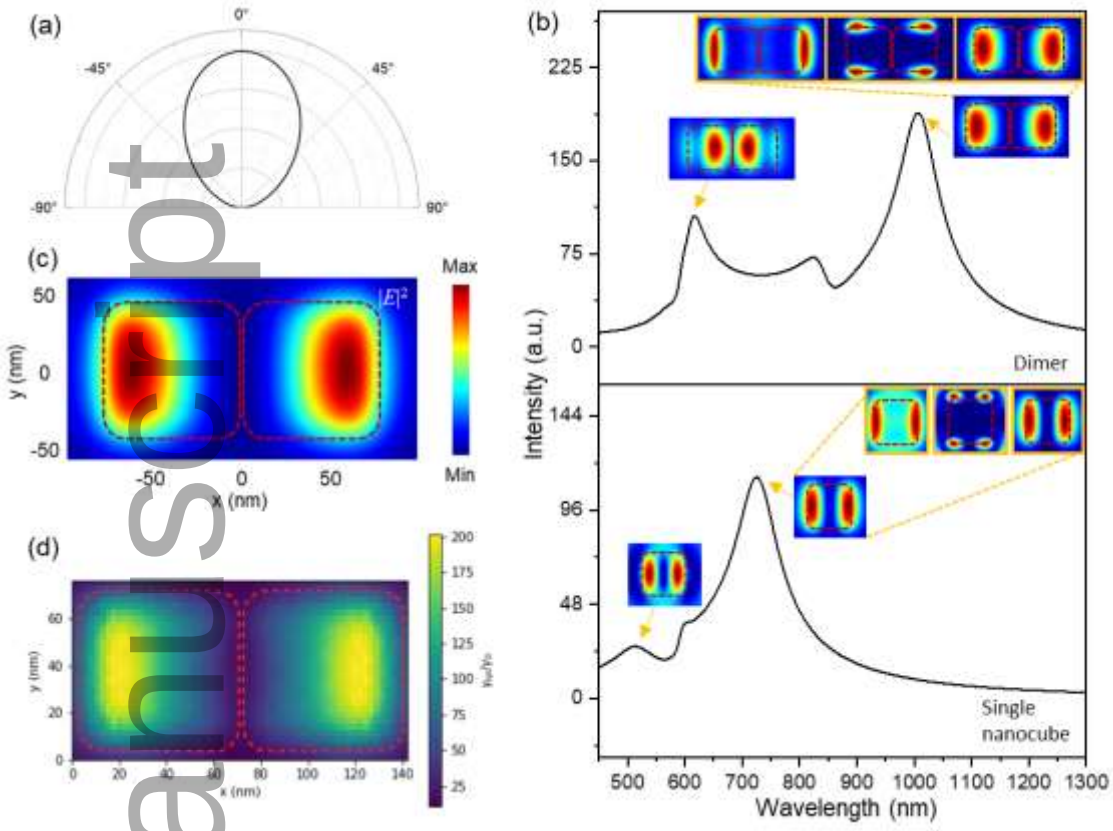

Figure 2. a) Simulated radiation pattern of the Au substrate-InSe flake-Ag nanocube dimer structure. b) Simulated resonance spectrum of the dimer structure (top) and the single nanocube structure (bottom). The inset images indicated with yellow arrows refer to the simulated electric field distribution of each indicated peak. The red dotted squares indicate the location of nanocubes. The simulated x-, y-, and z-electric field component of each peak is shown in the yellow box, sequentially from left, middle, and right respectively. c) Simulated map of the electric field distribution of the nanocube dimer. d) Simulated map of the Purcell factor of an emitter underneath the dimer structure.

Through finite-difference time-domain (FDTD) simulations, the radiation pattern of the AIAN structure is simulated to have its orientation normal to the Au substrate (**Figure 2a**). This shows that the AIAN structure has directionality, which increases collection efficiency, crucial when it comes to coupling with external optical environments. **Figure 2b** shows the simulated resonance spectrum of the structure. The inset images refer to the simulated electric field distribution of each indicated peak. It is notable that in the single nanocube structure, both resonance peaks show similar modes, whereas in the dimer structure (spacing of 5 nm owing to PVP layer), the electric field of the second resonance peak (~620 nm) is concentrated in the middle edge of the nanocubes. Each of the left, middle, and right yellow boxes in the inset images show the simulated x-, y-, and z-electric field distribution of each main peak, respectively. Given that the z-electric field distribution is similar to the total electric field distribution, it can be deduced that the electric field is largely dominated by the z-component, normal to the surface. Detailed information of the Fig. 2b is described in the Fig. s3. **Figure 2c** shows the simulated map of the electric field distribution of the nanocube dimer. It is shown that the mode is mostly concentrated on the side edge of each nanocube. **Figure 2d** shows the simulated result of the Purcell factor of the AIAN structure. As can be seen in **Figure 2d**, the spontaneous emission rate enhancement varies with respect to the spatial position of the region below the silver nanocube dimer. The maximum Purcell factor is ~200-fold and is calculated using the commercial FEM solver, COMSOL Multiphysics.

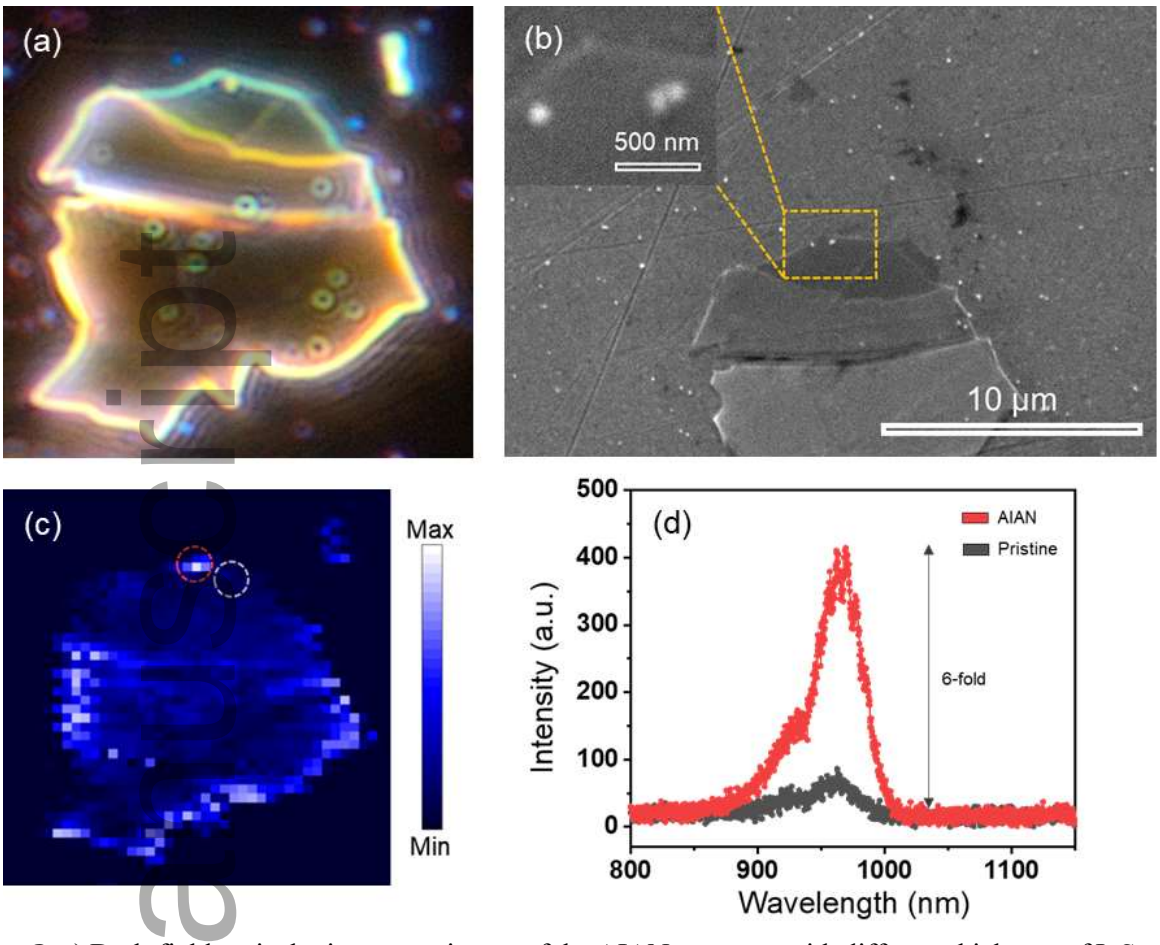

Figure 3. a) Dark-field optical microscopy image of the AlAN structure with different thickness of InSe across a flake. b) SEM image of the sample in (a). The inset shows the high-magnification SEM image of a single nanocube and dimer in the sample. c) PL intensity map of the sample in (a). The AlAN structure and pristine InSe region are indicated with red and grey circles respectively. d) Comparison of the measured PL spectrum between the AlAN structure and pristine InSe flake region on (c).

Figure 3a shows the dark-field optical microscopy image of the AlAN structure with different thicknesses of InSe flakes. The structure can be divided into three main regions with different thickness. The first region with green boundary has the thinnest InSe flake (~20 nm thick), and the following middle region has thickness of ~40 nm, and the bottommost, largest region has thickness of ~70 nm. The silver nanocubes can be observed in different modes in respect to the thickness of InSe below. Silver nanocubes on the thin flake (~20 nm) region are shown to have an Airy disk shape in the dark-field optical microscope, whereas on thicker flakes (above 40 nm thick) they have a donut shape. **Figure 3b** shows the SEM image of the sample in **Figure 3a**. The inset shows the high-magnification SEM image of a single nanocube and a dimer on the same flake. **Figure 3c** shows the PL intensity map of the sample in **Figure 3a**. The AlAN structure and the neighboring pristine InSe area without any silver nanocube on top are indicated with red and grey circles respectively. The bright PL is observed from the dimer location. The experimental light scattering spectrum showing intensity peak at InSe PL wavelength (Fig. s4) further reveals the resonance coupling between the InSe PL and plasmonic dimer structure. The double resonance modes in the light scattering spectrum are predicted to be caused by plasmon resonance coupling of two nanocubes, referred to as electrostatic coupling effects.[34,35] The single nanocube arrangement shows no enhancement compared to its surrounding areas. This is predicted due to the wavelength mismatch between the localized surface plasmon resonance (**Figure 2b**) and the InSe band edge PL. The AlAN structure with InSe flake thickness over 40 nm is shown to have no PL enhancement compared to its neighboring region without any Ag nanocubes. This is predicted to be caused by the weakened coupling strength caused by low proximity between two resonating metallic surfaces. This is expected to have decreased

light confinement strength. **Figure 3d** shows the PL spectra of InSe enhanced by plasmonic cavity effect from the AIAN structure and pristine InSe flake region in **Figure 3c**. The AIAN structure is shown to have a 6-fold PL enhancement compared to the pristine region of the same InSe flake on the gold substrate. The experimental enhancement factor is lower than theoretically predicted values. This is because experimentally we measure PL from extended area, which involves no plasmonic cavity affected region, that average enhancement can be measured, whereas in simulation was expressed with a point dipole source with local variation (25-200-fold). Other reasons are surface roughness and the non-optimal position of the structure in the experiment.

The boundary area of the middle and bottom region is shown to have brighter PL than the inner section of the same region. This is predicted to be due to distinct characteristic of thin flakes which can also be found in previous research.[18,36,37]

4. Conclusion

In this study, we demonstrate a plasmonic structure of a gold substrate, silver nanocube dimer, and a InSe layer in the gap region for PL enhancement. The simulation shows that the AIAN structure has directionality normal to the substrate and has two resonance spectrum peaks in the visible-NIR region. The maximum Purcell factor is shown on the short edge of the nanocube dimers. In the experimental analysis, it is found that it is possible to distinguish between thinner (~20 nm) and thicker (above 40 nm thick) InSe flakes, and the distribution of silver nanocubes, allowing the facile study of the overall morphology. The measured PL spectrum shows that the structure has an increase in the photoluminescence of ~6-fold at room temperature. The study paves the way for utilizing InSe for nanophotonic and optoelectronic devices.

Acknowledgements

This work was supported by the Melbourne Research Scholarship from the University of Melbourne. J.B. acknowledges financial support from the Australian Research Council (DE210101129). This work was performed in part at the Materials Characterization and Fabrication Platform (MCFP) at the University of Melbourne.

References

[1] J. R. Schaibley, H. Yu, G. Clark, P. Rivera, J. S. Ross, K. L. Seyler, W. Yao and X. Xu, *Nature Reviews Materials* **2016**, *1*, 16055.
[2] F. Xia, H. Wang, D. Xiao, M. Dubey and A. Ramasubramaniam, *Nat. Photonics* **2014**, *8*, 899.
[3] S. Kim, Y.-C. Lim, R. M. Kim, J. E. Fröch, T. N. Tran, K. T. Nam and I. Aharonovich, *Small* **2020**, *16*, 2003005.
[4] J. Yao, F. Chen, J. Li, J. Du, D. Wu, Y. Tian, C. Zhang, J. Yang, X. Li and P. Lin, *J. Mater. Chem. C* **2021**, *9*, 13123.
[5] L. A. Walsh and C. L. Hinkle, *Appl. Mater. Today* **2017**, *9*, 504.
[6] J. Zhang, F. Wang, V. B. Shenoy, M. Tang and J. Lou, *Materials Today* **2020**, *40*, 132.
[7] Y. Zhang, Y. Yao, M. G. Sendeku, L. Yin, X. Zhan, F. Wang, Z. Wang and J. He, *Adv. Mater.* **2019**, *31*, 1901694.
[8] W. Hao, C. Marichy and C. Journet, *2D Materials* **2018**, *6*, 012001.
[9] J. Cai, X. Han, X. Wang and X. Meng, *Matter* **2020**, *2*, 587.
[10]
[11] A. Afzalian, *npj 2D Materials and Applications* **2021**, *5*, 5.
[12] T. Hai, G. Xie, Z. Qiao, Z. Qin, J. Ma, Y. Sun, F. Wang, P. Yuan, J. Ma and L. Qian, *Nanophotonics* **2020**, *9*, 2045.
[13] G. W. Mudd, M. R. Molas, X. Chen, V. Zólyomi, K. Nogajewski, Z. R. Kudrynskyi, Z. D. Kovalyuk, G. Yusa, O. Makarovsky, L. Eaves, M. Potemski, V. I. Fal'ko and A. Patanè, *Sci. Rep.* **2016**, *6*, 39619.
[14] Y. Sun, Y. Li, T. Li, K. Biswas, A. Patanè and L. Zhang, *Adv. Funct. Mater.* **2020**, *30*, 2001920.
[15] D. A. Bandurin, A. V. Tyurnina, G. L. Yu, A. Mishchenko, V. Zólyomi, S. V. Morozov, R. K. Kumar, R. V. Gorbachev, Z. R. Kudrynskyi, S. Pezzini, Z. D. Kovalyuk, U. Zeitler, K. S. Novoselov, A. Patanè, L. Eaves, I. V. Grigorieva, V. I. Fal'ko, A. K. Geim and Y. Cao, *Nat. Nanotechnol.* **2017**, *12*, 223.
[16] J. F. Sánchez-Royo, G. Muñoz-Matutano, M. Brotons-Gisbert, J. P. Martínez-Pastor, A. Segura, A. Cantarero, R. Mata, J. Canet-Ferrer, G. Tobias, E. Canadell, J. Marqués-Hueso and B. D. Gerardot, *Nano Res.* **2014**, *7*, 1556.
[17] G. W. Mudd, S. A. Svatek, T. Ren, A. Patanè, O. Makarovsky, L. Eaves, P. H. Beton, Z. D. Kovalyuk, G. V. Lashkarev, Z. R. Kudrynskyi and A. I. Dmitriev, *Adv. Mater.* **2013**, *25*, 5714.
[18] M. Brotons-Gisbert, D. Andres-Penares, J. Suh, F. Hidalgo, R. Abargues, P. J. Rodríguez-Cantó, A. Segura, A. Cros, G. Tobias, E. Canadell, P. Ordejón, J. Wu, J. P. Martínez-Pastor and J. F. Sánchez-Royo, *Nano Lett.* **2016**, *16*, 3221.
[19] Z. Yang, W. Jie, C.-H. Mak, S. Lin, H. Lin, X. Yang, F. Yan, S. P. Lau and J. Hao, *ACS Nano* **2017**, *11*, 4225.
[20] Y.-R. Chang, P.-H. Ho, C.-Y. Wen, T.-P. Chen, S.-S. Li, J.-Y. Wang, M.-K. Li, C.-A. Tsai, R. Sankar, W.-H. Wang, P.-W. Chiu, F.-C. Chou and C.-W. Chen, *ACS Photonics* **2017**, *4*, 2930.
[21] C. Robert, D. Lagarde, F. Cadiz, G. Wang, B. Lassagne, T. Amand, A. Balocchi, P. Renucci, S. Tongay, B. Urbaszek and X. Marie, *Phys. Rev. B* **2016**, *93*, 205423.
[22] M. Palummo, M. Bernardi and J. C. Grossman, *Nano Lett.* **2015**, *15*, 2794.
[23] J. B. Lassiter, F. McGuire, J. J. Mock, C. Ciracì, R. T. Hill, B. J. Wiley, A. Chilkoti and D. R. Smith, *Nano Lett.* **2013**, *13*, 5866.
[24] G. M. Akselrod, C. Argyropoulos, T. B. Hoang, C. Ciracì, C. Fang, J. Huang, D. R. Smith and M. H. Mikkelsen, *Nat. Photonics* **2014**, *8*, 835.
[25] H. Yokoyama and K. Ujihara, *Spontaneous emission and laser oscillation in microcavities*, CRC press, **1995**.
[26] X.-W. Chen, M. Agio and V. Sandoghdar, *Physical Review Letters* **2012**, *108*, 233001.
[27] K. Kolasiński and B. Szafran, *Phys. Rev. B* **2013**, *88*, 165306.
[28] M. Brotons-Gisbert, R. Proux, R. Picard, D. Andres-Penares, A. Branny, A. Molina-Sánchez, J. F. Sánchez-Royo and B. D. Gerardot, *Nat. Commun.* **2019**, *10*, 3913.

[29] N. Mendelson, R. Ritika, M. Kianinia, J. Scott, S. Kim, J. E. Fröch, C. Gazzana, M. Westerhausen, L. Xiao, S. S. Mohajerani, S. Strauf, M. Toth, I. Aharonovich and Z.-Q. Xu, *Adv. Mater.* **2022**, *34*, 2106046.
[30] C. Viswanathan, G. Rusu, S. Gopal, D. Mangalaraj and S. Narayandass, *J. Optoelectron. Adv. Mater.* **2005**, *7*, 705.
[31] L. Novotny and B. Hecht, *Principles of nano-optics*, Cambridge university press, Cambridge, England **2012**.
[32] T. Zheng, Z. T. Wu, H. Y. Nan, Y. F. Yu, A. Zafar, Z. Z. Yan, J. P. Lu and Z. H. Ni, *RSC Advances* **2017**, *7*, 54964.
[33] M. R. Molas, A. V. Tyurnina, V. Zólyomi, A. K. Ott, D. J. Terry, M. J. Hamer, C. Yelgel, A. Babiński, A. G. Nasibulin, A. C. Ferrari, V. I. Fal'ko and R. Gorbachev, *Faraday Discussions* **2021**, *227*, 163.
[34] N. Grillet, D. Manchon, F. Bertorelle, C. Bonnet, M. Broyer, E. Cottancin, J. Lermé, M. Hillenkamp and M. Pellarin, *ACS Nano* **2011**, *5*, 9450.
[35] H. Chen, Z. Sun, W. Ni, K. C. Woo, H.-Q. Lin, L. Sun, C. Yan and J. Wang, *Small* **2009**, *5*, 2111.
[36] M. E. Pam, Y. Shi, J. Hu, X. Zhao, J. Dan, X. Gong, S. Huang, D. Geng, S. Pennycook, L. K. Ang and H. Y. Yang, *Nanoscale Advances* **2019**, *1*, 953.
[37] W. Ahmad, J. Liu, J. Jiang, Q. Hao, D. Wu, Y. Ke, H. Gan, V. Laxmi, Z. Ouyang, F. Ouyang, Z. Wang, F. Liu, D. Qi and W. Zhang, *Adv. Funct. Mater.* **2021**, *31*, 2104143.

This article illustrates the enhancement of photoluminescence (PL) from multi-layer InSe by inducing a gap plasmon between Ag nanocube dimer and an Au substrate. The simulated Purcell factor increases by a factor of 200. A 6-fold increase in PL relative to pristine InSe flake on an Au substrate is demonstrated experimentally at room temperature.